Bone 211 (2026) 117958

Contents lists available at ScienceDirect

Bone

journal homepage: www.elsevier.com/locate/bone

Full Length Article

Osteogenic promotion by naringin through the PI3K/AKT/mTOR pathway-mediated activation of autophagy and inhibition of apoptosis

Yubo Cui [a,1], Guisong Yu [a,c,1], Dian Li [a,b], Xing Fu [a], Zhijun Yang [b], Wenlong Yang [b], Fengyun Yang [b,*]

[a] Jiangxi University of Chinese Medicine, Nanchang, 330000, Jiangxi, China
[b] Affiliated Hospital of Jiangxi University of Chinese Medicine, Nanchang, 330000, Jiangxi, China
[c] The First Affiliated Hospital of Lishui University, China

ARTICLE INFO

Keywords:
Osteoporosis
Autophagy
Apoptosis
Naringin

ABSTRACT

Osteoporosis is a common age-related metabolic bone disease closely associated with osteoblast dysfunction, abnormal apoptosis, and dysregulated autophagy. Naringin, a dihydroflavonoid compound mainly found in citrus fruits and various traditional Chinese medicinal herbs (e.g., *Aurantii Fructus Immaturus* and *Rhizoma Drynariae*), exhibits potential anti-aging and osteoprotective effects; however, its specific mechanism requires systematic elucidation. Network pharmacology analysis revealed that the core targets of naringin are significantly enriched in the PI3K/AKT signaling pathway, as well as pathways related to apoptosis and autophagy. Subsequent in vitro experiments demonstrated that naringin promotes osteoblast proliferation, differentiation, and mineralization; upregulates the expression of osteogenic markers; activates protective autophagy; and inhibits apoptosis. By employing the autophagy inhibitor 3-MA and the PI3K/AKT agonist 740Y-P to modulate PI3K/AKT/mTOR-mediated autophagy, we confirmed that the anti-apoptotic effect of naringin is dependent on the activation of autophagy. In vivo, naringin administration inhibited the excessive activation of the PI3K/AKT/mTOR pathway, enhanced autophagy, suppressed excessive apoptosis, ameliorated bone microarchitecture, and increased bone mineral density in ovariectomized mice. Our findings elucidate the mechanism by which naringin exerts its anti-osteoporotic effects through regulating the balance between autophagy and apoptosis, thereby providing a theoretical basis for developing naringin-based anti-aging strategies for bone protection.

1. Introduction

Osteoporosis (OP) is a systemic metabolic bone disease characterized by decreased bone mass, deterioration of bone microstructure, and increased fracture risk, which predisposes patients to fragility fractures under low-energy impact (e.g., from a fall or even coughing) [1]. Epidemiological data indicate that the prevalence of OP in China is approximately 20.3%, rising significantly with age: 35.2% among individuals aged 60–69 years, 44.1% in those aged 70–79 years, and 53.9% in the population aged 80 years and above [2]. The core pathological mechanism of OP involves an imbalance in bone remodeling, where bone resorption exceeds bone formation. In this process, reduced osteoblast proliferation and differentiation capacity, coupled with excessive apoptosis, are key factors leading to inadequate bone formation and subsequent osteoporosis [3,4].

Current first-line clinical treatments primarily include bisphosphonates and receptor activator of nuclear factor-κB ligand (RANKL) inhibitors. These agents exert their therapeutic effect predominantly by inhibiting osteoclast activity and reducing bone resorption [5,6]. However, long-term use of these drugs is associated with potential adverse effects, such as osteonecrosis of the jaw, atypical femoral fractures, and hypocalcemia, which may limit their clinical utility [7,8]. Consequently, discovering highly effective, low-toxicity, and multi-targeting bone-forming agents from natural products has become a major focus in osteoporosis research.

Naringin (Nar) is a flavonoid abundant in citrus fruits and certain traditional Chinese medicines, such as *Citrus aurantium* (bitter orange) and *Drynaria fortunei*. Studies have identified that Nar possesses diverse pharmacological activities, including anti-inflammatory, antioxidant, and cardiovascular protective effects [9,10]. In recent years, growing

* Corresponding author at: No. 425, Baizhadao, Nanchang City, Jiangxi Province, China.
E-mail address: yfy_jxszyy@126.com (F. Yang).
[1] These authors contributed equally to this work.

https://doi.org/10.1016/j.bone.2026.117958
Received 27 February 2026; Received in revised form 28 May 2026; Accepted 2 June 2026
Available online 2 June 2026
8756-3282/© 2026 Elsevier Inc. All rights are reserved, including those for text and data mining, AI training, and similar technologies.

Descargado para Lucia Angulo (lu.maru26@gmail.com) en National Library of Health and Social Security de ClinicalKey.es por Elsevier en octubre 15, 2026. Para uso personal exclusivamente. No se permiten otros usos sin autorización. Copyright ©2026. Elsevier Inc. Todos los derechos reservados.

evidence has revealed its significant beneficial effects on the skeletal system [11]. Naringin can promote the osteogenic differentiation of bone marrow mesenchymal stem cells (BMSCs), markedly enhance alkaline phosphatase (ALP) activity, and accelerate the formation of mineralized nodules [12,13]. Furthermore, experimental studies have demonstrated that naringin can upregulate the expression of osteogenesis-related proteins, effectively counteract ovariectomy (OVX)-induced osteoporosis, and exert a clear protective effect on bone in animal models. Its mechanism of action in regulating bone metabolism involves multiple signaling pathways, such as phosphatidylinositol 3-kinase/protein kinase B (PI3K/AKT), c-Fos/c-Jun, AMP-activated protein kinase (AMPK), and Wnt/β-catenin [14,15].

Autophagy is a highly conserved intracellular degradation and recycling system. In this process, damaged organelles or proteins are enveloped by forming autophagosomes, which subsequently fuse with lysosomes for degradation, thereby maintaining intracellular homeostasis and providing energy [16–18]. In osteoblasts, a moderate level of autophagy has been confirmed to be essential for maintaining their survival, differentiation, and function. It facilitates the clearance of damaged mitochondria and other organelles, reduces oxidative and endoplasmic reticulum stress, and consequently inhibits osteoblast apoptosis [19,20]. The PI3K/AKT/mTOR signaling pathway serves as a central regulator of cell growth, metabolism, and autophagy. Activation of the PI3K/AKT pathway leads to phosphorylation and activation of its downstream effector mTOR, which in turn suppresses autophagy initiation [21,22]. Therefore, a key scientific question remains to be elucidated: whether naringin promotes osteogenic function and inhibits osteoblast apoptosis by activating protective autophagy through modulation of the PI3K/AKT/mTOR signaling.

This study aims to systematically investigate the effects of naringin on osteoblast proliferation, differentiation, apoptosis, and autophagy, and to elucidate its role in mitigating osteoporosis via the PI3K/AKT/mTOR signaling pathway. The findings are expected to provide a theoretical foundation for developing naringin as a natural therapeutic agent and to offer novel insights for future osteoporosis research.

2. Materials and methods

2.1. Materials

Naringin (purity ≥98%) was obtained from Beijing Solaibao Technology Co., Ltd. The MC3T3-E1 Subclone 14 pre-osteoblast cell line was acquired from Wuhan Punosay Life Technology Co., Ltd. The Cell Counting Kit-8 (CCK-8) and alizarin red staining kit were sourced from Beijing Solaibao Technology Co., Ltd. The Annexin V-FITC/PI apoptosis detection kit was procured from Wuhan Servicebio Biotechnology Co., Ltd. The BCA protein assay kit was supplied by Beijing ComWin Biotech Co., Ltd. Antibodies against the following proteins were purchased from Wuhan Sanying Biotechnology Co., Ltd.: PI3K, p-PI3K, AKT, p-AKT, mTOR, p-mTOR, cleaved Caspase-3, LC3B, p62, Beclin-1, BAX, and Bcl-2.

2.2. Network pharmacological analysis

The two-dimensional chemical structure of naringin was retrieved from the PubChem database and submitted to the SwissTargetPrediction, TCMSP, and PharmMapper databases to predict its potential targets. Disease targets associated with osteoporosis were identified by searching the OMIM, DisGeNET, and GeneCards databases using "osteoporosis" as the keyword. The JVENN online tool was then employed to generate a Venn diagram and obtain the intersection between the drug and disease targets, which were defined as the core therapeutic targets of naringin against osteoporosis. Subsequently, Gene Ontology (GO) functional enrichment and Kyoto Encyclopedia of Genes and Genomes (KEGG) pathway enrichment analyses were performed on these intersection targets using the Metascape database. The results were visualized as bar and bubble charts via the online bioinformatics platform (bioinformatics.com.cn). Finally, molecular docking simulation was conducted to validate the interactions. The three-dimensional structures of the core target proteins were downloaded in PDB format from the Protein Data Bank (PDB). The SDF-format file of naringin was obtained from PubChem. Docking simulations were performed using AutoDockTools 1.5.6 software, and the results were visualized with PyMOL.

2.3. Cell culture

MC3T3-E1 pre-osteoblasts were cultured in a humidified incubator at 37 °C with 5% CO_2. The culture medium was replenished every 48 to 72 h. Upon reaching approximately 90% confluence, cells were rinsed twice with phosphate-buffered saline (PBS) and then detached using trypsin-EDTA solution. After neutralizing the trypsin with complete medium, the cells were subcultured at a 1:3 split ratio. For subsequent experiments, cells in the exponential growth phase were harvested to prepare a single-cell suspension. The suspension was then seeded into 6-well or 12-well plates at predetermined densities to establish the required cellular models.

2.4. Cell viability assay (CCK-8)

MC3T3-E1 cells were seeded in 96-well plates at a density of 5×10^3 cells per well and allowed to adhere overnight. The cells were then treated with naringin at various concentrations. After 12, 24, and 48 h of treatment, 10 μL of CCK-8 reagent was added to each well, and the plates were incubated for an additional 2 h at 37 °C. Finally, the absorbance of each well was measured at 450 nm using a microplate reader to determine cell viability.

2.5. Alkaline phosphatase (ALP) staining

MC3T3-E1 cells were seeded in 6-well plates. After 24 h, the culture medium was replaced with osteogenic induction medium containing different concentrations of naringin. Following 14 days of induction, the cells were fixed and stained for ALP activity according to the manufacturer's protocol. The stained mineralized nodules were observed and photographed under an inverted microscope (OLYMPUS IX71). For quantitative analysis, the stained areas were quantified using ImageJ software.

2.6. Alizarin Red S staining

To assess extracellular matrix mineralization, MC3T3-E1 cells were cultured in osteogenic induction medium supplemented with different concentrations of naringin for 35 days. The medium was refreshed every 3–4 days. After the induction period, cells were fixed and stained with Alizarin Red S solution according to the manufacturer's protocol. The formation of calcified nodules was observed and photographed under an inverted microscope.

2.7. Immunofluorescence staining

MC3T3-E1 cells seeded in 12-well plates were treated with naringin at specified concentrations for the desired duration. Subsequently, the cells were fixed with 4% paraformaldehyde at room temperature for 30 min and permeabilized with 0.5% Triton X-100 in PBS for 15 min. After blocking with 5% bovine serum albumin (BSA) for 1 h at room temperature, the cells were incubated overnight at 4 °C with the appropriate primary antibody diluted in blocking buffer. Following three washes with PBS, the cells were incubated with fluorochrome-conjugated secondary antibodies in the dark for 1 h at room temperature. Cell nuclei were counterstained with DAPI. Finally, fluorescent images were captured using an inverted fluorescence microscope and analyzed with

Descargado para Lucia Angulo (lu.maru26@gmail.com) en National Library of Health and Social Security de ClinicalKey.es por Elsevier en octubre 15, 2026. Para uso personal exclusivamente. No se permiten otros usos sin autorización. Copyright ©2026. Elsevier Inc. Todos los derechos reservados.

ImageJ software.

2.8. Analysis of apoptosis by flow cytometry

MC3T3-E1 cells were seeded in 6-well plates. After 24 h, the cells were treated with various concentrations of naringin for a specified duration. After treatment, both the culture supernatant and the cells detached by trypsinization (without EDTA) were collected and centrifuged. The cells were gently resuspended in pre-chilled 1× Binding Buffer and adjusted to a density of 1–5 × 10^6 cells/mL. For staining, 500 μL of the cell suspension was mixed with 5 μL of Annexin V-FITC and 5 μL of PI. After incubation in the dark at room temperature for 15 min, the samples were analyzed immediately using a flow cytometer (FONGCYTE C2060).

2.9. Analysis of mRFP-GFP-LC3 fluorescence

Cells were transduced with the autophagy double-labeled lentivirus mRFP-EGFP-LC3B to monitor autophagic flux. At 24 h post-transduction, cells were treated with the indicated drugs. Fluorescence images were randomly captured from each group using a confocal laser scanning microscope (Leica STELLARIS 5). Yellow puncta represented autophagosomes, while red puncta represented autolysosomes. The number of autophagic puncta per cell was quantified using ImageJ software, with at least 100 intact cells analyzed per group. Autophagic flux was evaluated by calculating the ratio of autophagosomes to autolysosomes.

2.10. Observation of autophagic vacuoles by monodansylcadaverine (MDC) staining

After treatment with naringin, the culture medium was removed from the 6-well plates. The cells were washed three times with PBS and then incubated with 1 mL of MDC staining working solution (1×) per well at 37 °C in the dark for 30 min. Subsequently, the staining solution was removed, and the cells were washed three times with PBS. Autophagic vacuoles, which exhibit bright green fluorescence, were observed and imaged under a fluorescence microscope. Fluorescence intensity can be quantified using image analysis software such as ImageJ.

2.11. Animal model and treatment

Forty female C57BL/6 mice (8 weeks old) were purchased from Jiangsu Huachuang Sino Medic Technology Co., Ltd. (Production License: SCXK(Su) 2020-0009). The mice were housed in the specific pathogen-free animal facility of Jiangxi University of Traditional Chinese Medicine under controlled conditions: temperature 22 ± 1 °C, humidity 55 ± 5%, and a 12-hour light/dark cycle, with free access to food and water. All animal procedures were approved by the Animal Ethics Committee of Jiangxi University of Traditional Chinese Medicine (Approval No.: JZLLSC20250615). All experiments were performed in accordance with the relevant guidelines and regulations. The authors complied with the ARRIVE guidelines.

After one week of acclimatization, osteoporosis was induced via bilateral ovariectomy (OVX) under anesthesia. Mice in the sham-operated group underwent the same surgical procedure except for ovary removal. One week post-surgery, the mice were randomly assigned to five groups: (1) Sham group, (2) OVX model group, (3) OVX + alendronate sodium (ALN, 1.3 mg/kg/day), (4) OVX + naringin (300 mg/kg/day), and (5) OVX + naringin (150 mg/kg/day). ALN and naringin were suspended in normal saline and administered daily by oral gavage for 12 consecutive weeks. Mice in the Sham and OVX groups received an equal volume of vehicle (normal saline). After the 12-week treatment period, all mice were euthanized under deep anesthesia. Blood samples were collected, and femurs were dissected, cleaned of soft tissue, and stored at −80 °C for subsequent analysis.

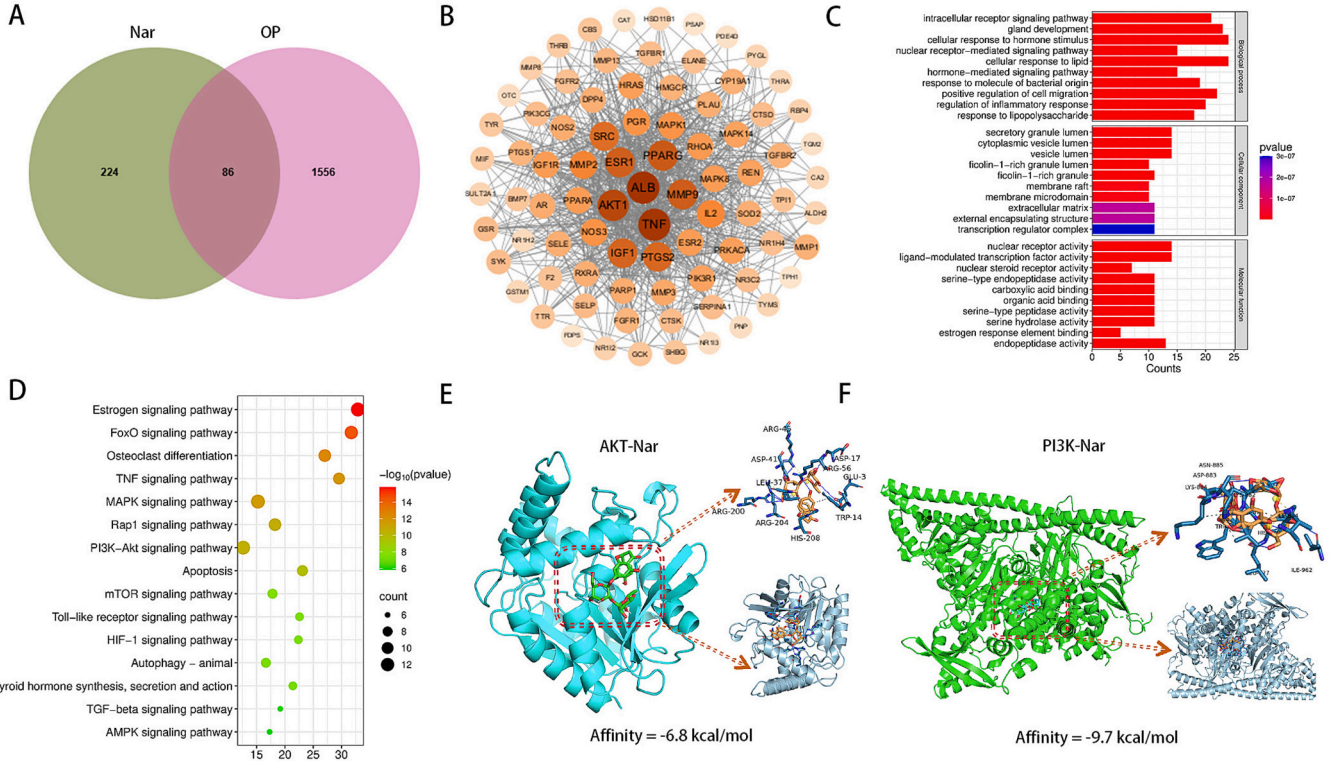


Fig. 1. Network pharmacology and molecular docking of naringin in the treatment of osteoporosis. **A:** Intersection of targets of naringin and OP-related targets; **B:** PPI of naringin for osteoporosis; **C–D:** Metascape database was used for GO and KEGG enrichment analysis; **E–F:** Molecular docking simulation of naringin with AKT and PI3K,respectively.

Descargado para Lucia Angulo (lu.maru26@gmail.com) en National Library of Health and Social Security de ClinicalKey.es por Elsevier en octubre 15, 2026. Para uso personal exclusivamente. No se permiten otros usos sin autorización. Copyright ©2026. Elsevier Inc. Todos los derechos reservados.

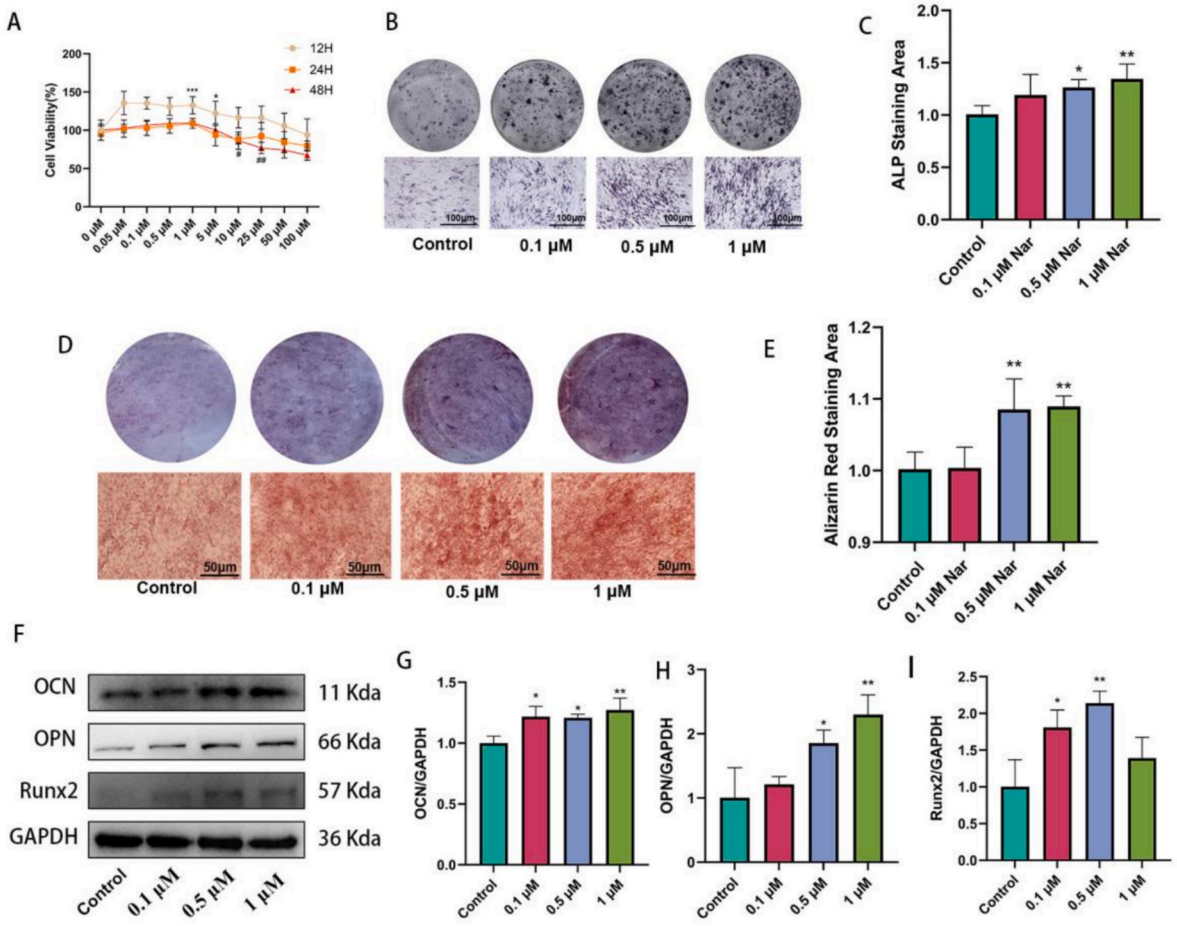


Fig. 2. Naringin promoted the proliferation and osteogenic differentiation of MC3T3-E1 cells. **A:** CCK-8 was used to detect the effect of naringin on cell viability (n = 9). **B–C:** Different concentrations of naringin in intervened cells, ALP activity was observed under a microscope (n = 4); **D–E:** Different concentrations of naringin in intervened cells, and the mineralized nodules of osteoblasts were observed under a microscope (n = 4). **F–I:** After intervention with naringin, the expression of osteogenic-related proteins was promoted (n = 3). * $P < 0.05$, ** $P < 0.01$, ***$P < 0.001$ compared with control.

2.12. Micro-CT analysis

The femoral tissue was scanned using Micro CT (Lifeporetech VNC-102). The original images were reconstructed with the 3D reconstruction software Recon. The data analysis software Avatar was used to analyze the ROI of the target region, and the same region of interest was selected across all samples to obtain the required parameter values and export the data.

2.13. Histological and immunohistochemical staining analysis

The femur was fixed in 4% paraformaldehyde for 48 h and decalcified in EDTA for 14 days. After decalcification, 4-μm sections were prepared through dehydration in a gradient of ethanol, clearing in xylene, and embedding in paraffin. For HE staining, the sections were deparaffinized and rehydrated, stained with hematoxylin for 5 min, differentiated with acid alcohol, blued with tap water, and stained with eosin for 2 min. After dehydration and clearing, the sections were mounted with neutral gum and observed under a light microscope. For IHC staining: After deparaffinization and rehydration, the sections underwent antigen retrieval with citrate antigen repair solution for 15 min, were incubated with 3% H_2O_2 at room temperature for 10 min, rinsed with PBS, blocked with 5% BSA at 37 °C for 30 min, and incubated with the primary antibody at 4 °C overnight. The next day, the secondary antibody was incubated at 37 °C for 50 min. Color was developed with DAB in the dark for 5 min, and the sections were then photographed under a microscope for observation.

2.14. Western blot analysis

Protein extracted from femoral tissue and cells was mixed with 5× loading buffer (at a volume ratio of 4:1) and the mixture was boiled at 100 °C for 10 min. For each sample, 50 μg of protein was electrophoresed and transferred to a PVDF membrane. The membrane was incubated with primary antibody (dilution ratio 1:1000) overnight at 4 °C. Subsequently, it was incubated with secondary antibody (diluted 1:10,000) for 1 h at room temperature. Protein bands were visualized using ECL chemiluminescence. The band intensities of target proteins were quantified using ImageJ software, with GAPDH as the reference.

2.15. Statistical analysis

All data were analyzed using GraphPad Prism (version 10) and are presented as the mean ± standard deviation. Comparisons among groups were made by one-way analysis of variance. A *P*-value of less than 0.05 ($P < 0.05$) was considered statistically significant.

3. Results

3.1. Network pharmacology predicts the involvement of PI3K/AKT/mTOR pathway in naringin's effects on autophagy and apoptosis in osteoporosis

To elucidate the potential mechanisms of naringin against osteoporosis, a network pharmacology approach was employed. The two-

Descargado para Lucia Angulo (lu.maru26@gmail.com) en National Library of Health and Social Security de ClinicalKey.es por Elsevier en octubre 15, 2026. Para uso personal exclusivamente. No se permiten otros usos sin autorización. Copyright ©2026. Elsevier Inc. Todos los derechos reservados.

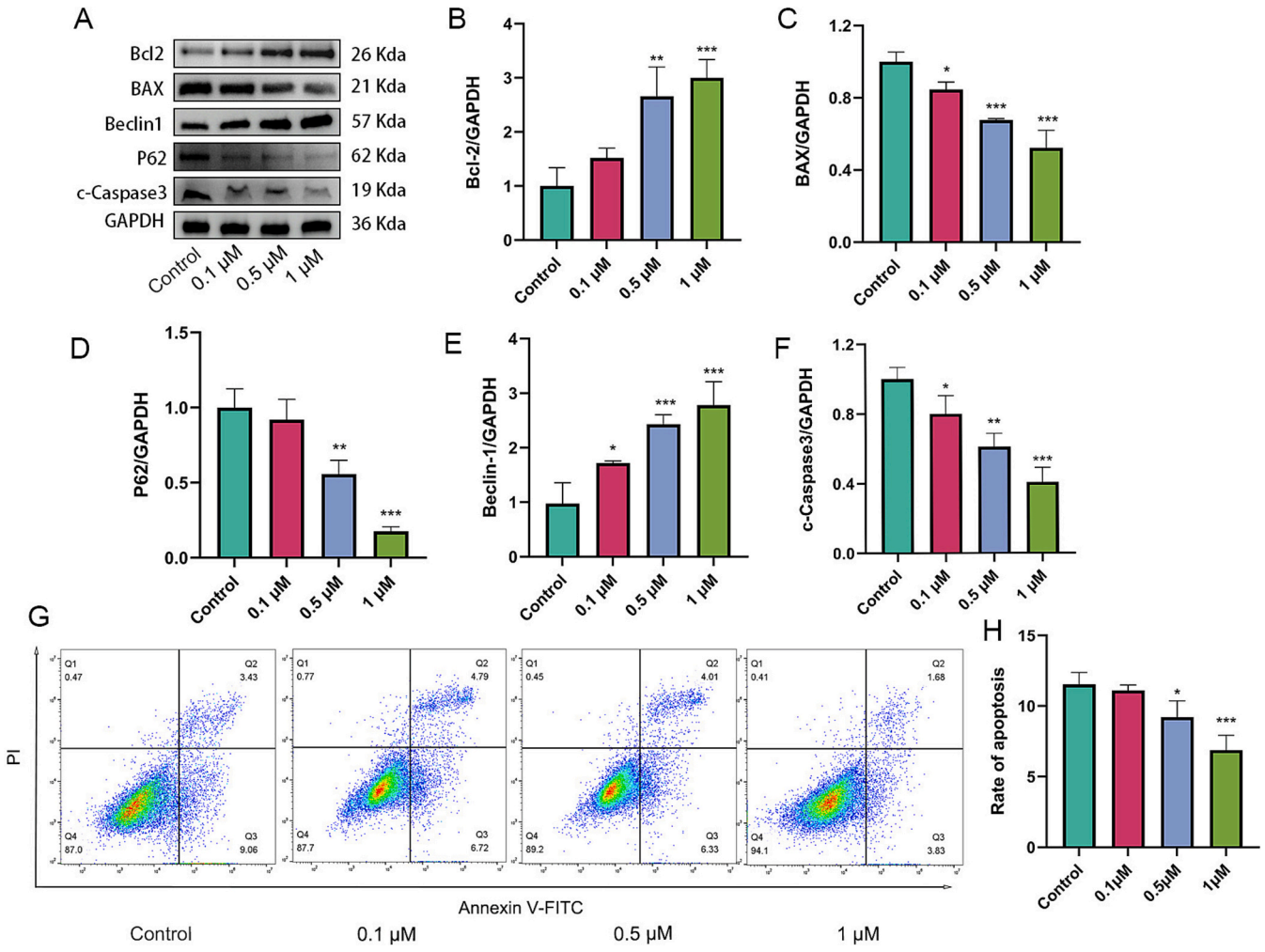


Fig. 3. Naringin activated autophagy and inhibited apoptosis in MC3T3-E1 cells (n = 3). **A–F:** Expression of autophagy - and apoptosis-related proteins after naringin intervention; **G–H:** Flow cytometry was used to detect the apoptosis rate of MC3T3-E1 cells after naringin intervention. * $P < 0.05$, ** $P < 0.01$, ***$P < 0.001$ compared with control.

dimensional structure of naringin was retrieved from the PubChem database. Potential targets of naringin were predicted using the SwissTargetPrediction, PharmMapper, and TCMSP databases, yielding 310 unique targets. Meanwhile, 1642 osteoporosis (OP)-related targets were collected from the OMIM, DisGeNET, and GeneCards databases. The intersection of these two target sets identified 86 common targets (Fig. 1A), which were considered potential therapeutic targets of naringin for OP. Subsequently, these 86 core targets were submitted to the STRING database to construct a protein-protein interaction (PPI) network. The interaction data were then imported into Cytoscape software for visualization and analysis. Nodes in the network were color-coded based on their degree value (Fig. 1B). Targets represented by nodes with darker colors possess higher connectivity, suggesting their potential key roles in the therapeutic mechanism of naringin for OP.

To identify the regulatory effects of naringin on signaling pathways associated with the core targets, GO and KEGG enrichment analyses were performed using the Metascape database. The enriched biological processes primarily included intracellular receptor signaling, cellular response to hormone stimulus, hormone-mediated signaling pathway, and regulation of inflammatory response. Cellular component terms were mainly related to secretory granule lumen, vesicle lumen, membrane raft, and extracellular matrix. Molecular functions involved nuclear receptor activity, ligand-activated transcription factor activity, and steroid hormone receptor activity (Fig. 1C). KEGG analysis was performed, and after excluding pathways unrelated to osteoporosis, multiple bone metabolism signaling pathways were enriched and ranked by *P* value. These pathways were predominantly enriched in categories related to osteoblast proliferation and apoptosis, autophagic homeostasis, osteoclast differentiation, inflammatory and immune responses, calcium and phosphorus metabolism, and osteogenic repair. We therefore speculate that naringin may exert its anti-osteoporosis effects by modulating autophagy and apoptosis mediated by the PI3K/AKT/mTOR signaling pathway (Fig. 1D).

Moreover, we observed that AKT1 and PIK3R1 ranked among the top potential therapeutic targets and were enriched in pathways related to PI3K/AKT signaling. Therefore, molecular docking simulations were conducted between naringin (as a small-molecule ligand) and the protein structures of AKT1 and PIK3R1 (Fig. 1E). The results showed that naringin exhibited binding affinities lower than −5.0 kcal/mol for both receptors, indicating favorable binding activity with these target proteins.

3.2. *Naringin promotes the proliferation and differentiation of MC3T3-E1 osteoblasts*

The effect of naringin on osteoblast proliferation and differentiation was investigated. MC3T3-E1 cells were treated with various concentrations of naringin (0.05–100 μmol/L) for 12, 24, and 48 h, and cell viability was assessed using the CCK-8 assay. The results showed that naringin at concentrations of 0.1–1 μmol/L significantly promoted cell

Descargado para Lucia Angulo (lu.maru26@gmail.com) en National Library of Health and Social Security de ClinicalKey.es por Elsevier en octubre 15, 2026. Para uso personal exclusivamente. No se permiten otros usos sin autorización. Copyright ©2026. Elsevier Inc. Todos los derechos reservados.

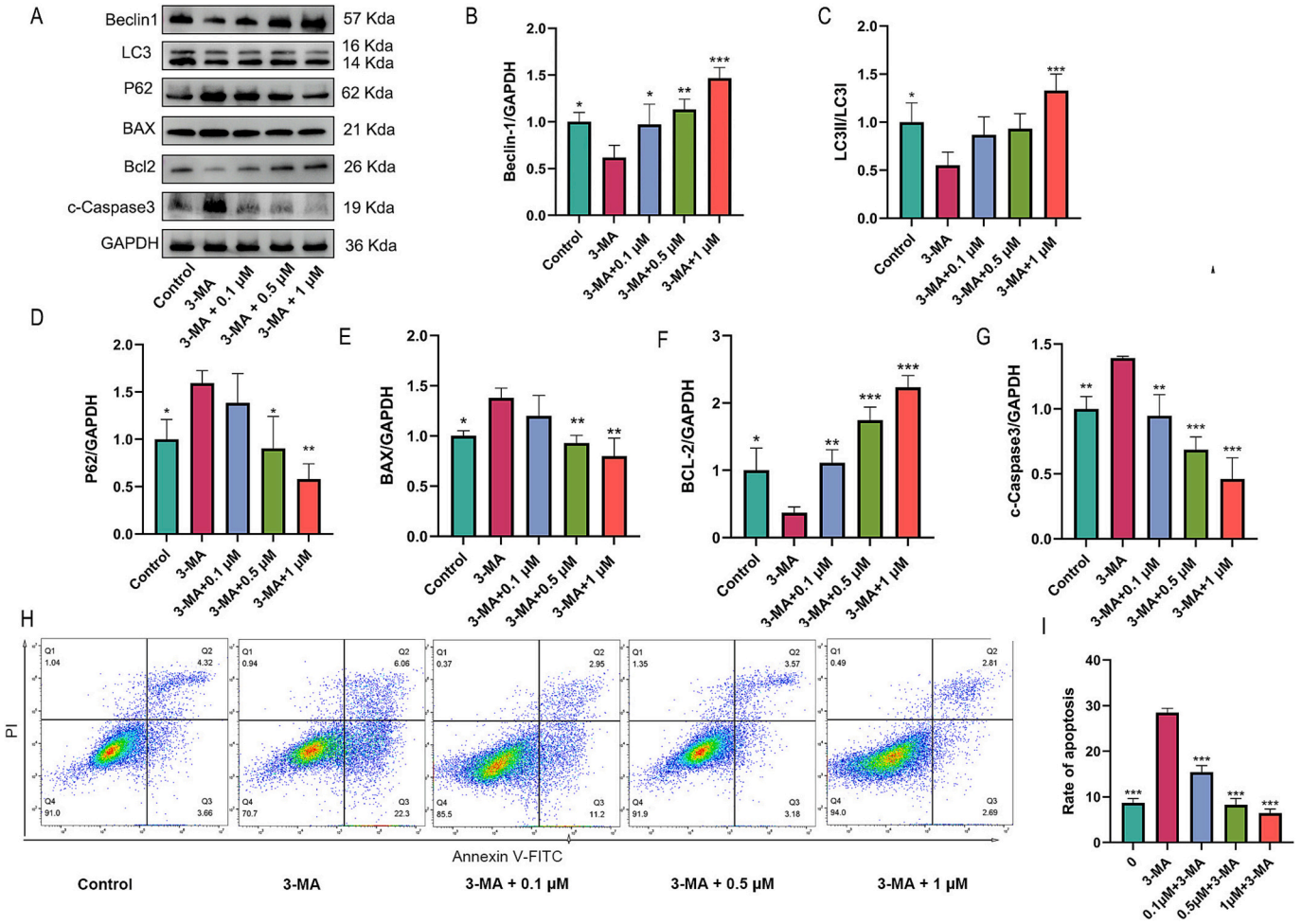


Fig. 4. Naringin intervention reversed 3-MA-mediated autophagy inhibition, reactivated autophagy, and inhibited apoptosis in MC3T3-E1 cells (n = 3). **A–G:** The expression of autophagy - and apoptosis-related proteins after the intervention of naringin and 3-MA; **H–I:** The apoptosis rate of MC3T3-E1 cells was detected by flow cytometry. * $P < 0.05$, ** $P < 0.01$, ***$P < 0.001$ compared with control.

proliferation, with 1 μmol/L exhibiting the most potent effect (Fig. 2A). To evaluate osteogenic differentiation, cells were treated with 0.1–1 μmol/L naringin for 14 days. ALP staining revealed a dose-dependent increase in staining intensity compared to the control group, indicating enhanced ALP activity (Fig. 2B, C). Similarly, Alizarin Red S staining demonstrated that naringin significantly promoted the formation of mineralized nodules. The staining intensity and nodule maturity increased with higher naringin concentrations (Fig. 2D, E). Furthermore, Western blot analysis was performed to detect the expression of osteogenic markers. The protein levels of runt-related transcription factor 2 (RUNX2), osteopontin (OPN), and osteocalcin (OCN) were significantly upregulated in naringin-treated MC3T3-E1 cells compared to controls (Fig. 2F–I).

3.3. Naringin promotes autophagy and inhibits apoptosis in MC3T3-E1 cells

The effects of naringin on osteoblast apoptosis and autophagy were examined. Western blot analysis showed that naringin treatment downregulated the expression of pro-apoptotic proteins (cleaved Caspase-3 and BAX) while upregulating the anti-apoptotic protein Bcl-2. Furthermore, naringin intervention significantly increased the level of the autophagy-related protein Beclin1 and decreased the level of the autophagy substrate P62, indicating activation of autophagy (Fig. 3A–F). Flow cytometry analysis confirmed that naringin significantly inhibited osteoblast apoptosis (Fig. 3G, H).

To investigate whether the anti-apoptotic effect of naringin depends on autophagy activation, cells were co-treated with the autophagy inhibitor 3-methyladenine (3-MA, 5 mmol/L). 3-MA treatment effectively suppressed autophagy, as evidenced by a decreased LC3-II/I ratio and Beclin1 expression, alongside increased P62 expression. Concurrently, 3-MA promoted osteoblast apoptosis, characterized by upregulated cleaved Caspase-3 and BAX, and downregulated Bcl-2. Notably, naringin co-treatment reversed these 3-MA-induced effects, reactivating autophagy and inhibiting apoptosis in a dose-dependent manner (Fig. 4A–G). Flow cytometry results were consistent with the protein expression data: 3-MA increased the apoptosis rate, and naringin effectively counteracted this increase (Fig. 4H, I). These findings were further validated by immunofluorescence and MDC staining (Fig. 5A–D).

3.4. Naringin regulates autophagy and apoptosis in MC3T3-E1 cells via the PI3K/AKT/mTOR pathway

To investigate whether the PI3K/AKT/mTOR pathway mediates the effects of naringin on autophagy and apoptosis, MC3T3-E1 cells were co-treated with naringin and the specific PI3K activator 740Y-P (20 μmol/L) [23]. Treatment with 740Y-P alone significantly increased the phosphorylation levels of PI3K, AKT, and mTOR (Fig. 6A–D), while downregulating the expression of Bcl-2, the LC3-II/LC3-I ratio, and Beclin-1, and upregulating p62, cleaved caspase-3, and BAX. Co-treatment with naringin significantly reversed these alterations, promoting autophagy and inhibiting apoptosis (Fig. 6E–K). Flow cytometry analysis yielded

Descargado para Lucia Angulo (lu.maru26@gmail.com) en National Library of Health and Social Security de ClinicalKey.es por Elsevier en octubre 15, 2026. Para uso personal exclusivamente. No se permiten otros usos sin autorización. Copyright ©2026. Elsevier Inc. Todos los derechos reservados.

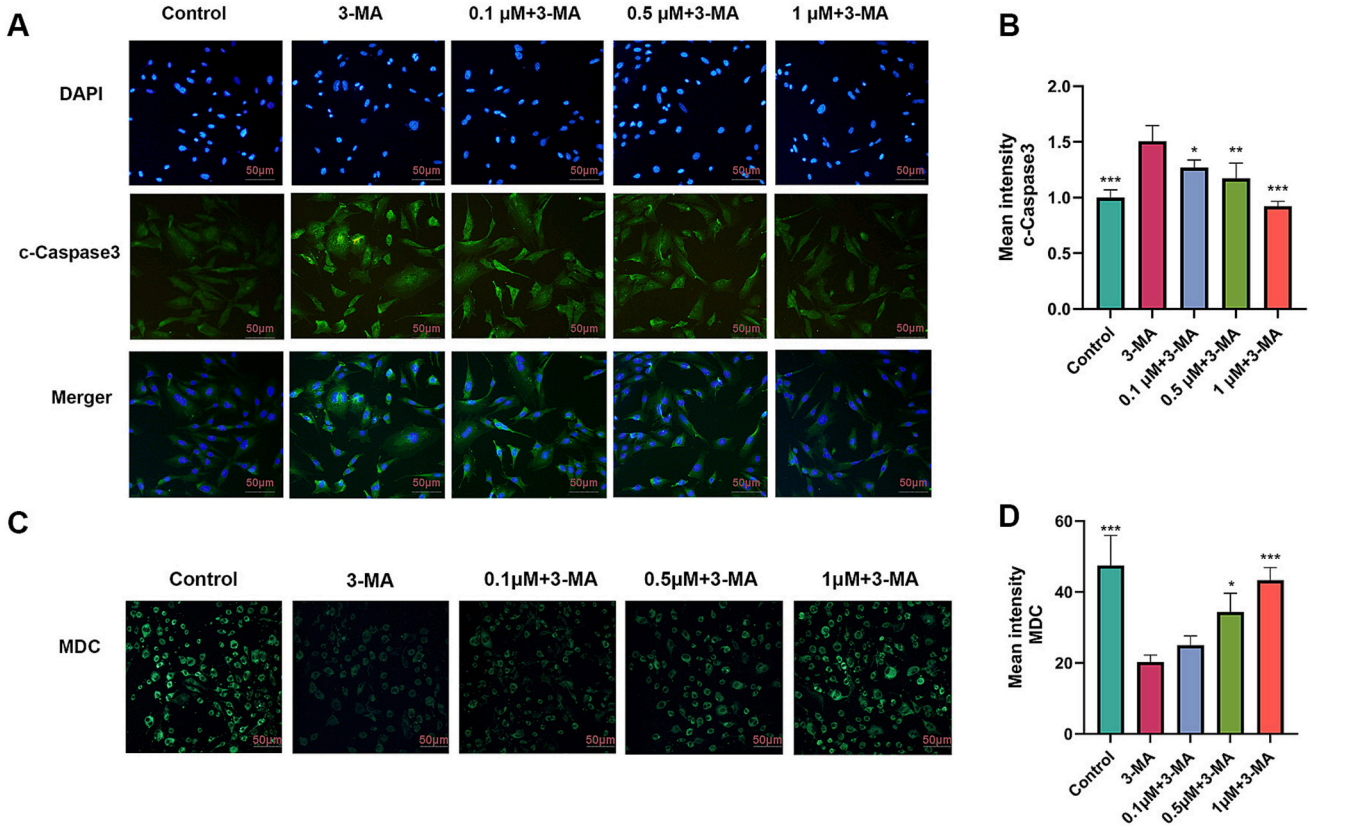


Fig. 5. Naringin intervention reversed 3-MA-mediated autophagy inhibition, reactivated autophagy, and inhibited apoptosis in MC3T3-E1 cells (n = 3). **A–B:** c-Caspase3 protein was detected by immunofluorescence staining; **C–D:** MDC method was used to detect the level of autophagy. * $P < 0.05$, ** $P < 0.01$, ***$P < 0.001$ compared with control.

results consistent with the protein expression data: 740Y-P markedly increased the apoptosis rate, an effect that was effectively attenuated by naringin (Fig. 7A). MDC staining showed that 740Y-P treatment reduced autophagic fluorescence intensity, indicating suppressed autophagy, and co-treatment with naringin reversed this reduction, restoring autophagic activity (Fig. 7B). Furthermore, autophagic flux was evaluated using mRFP-GFP-LC3 dual-fluorescence labeling, with the ratio of red to yellow puncta serving as an indicator of autophagic flux activity. Following 740Y-P treatment, the red-to-yellow ratio decreased, indicating inhibited autophagic flux; co-treatment with naringin significantly increased this ratio, effectively activating autophagic flux, which corroborated the aforementioned results (Fig. 7C).

3.5. Naringin alleviates osteoporosis in ovariectomized mice

To evaluate the in vivo protective effect of naringin against osteoporosis, a mouse model was established by bilateral ovariectomy (OVX). Micro-CT analysis revealed a significant deterioration of trabecular bone microstructure in the OVX group compared to the sham-operated group. Intervention with the positive control drug alendronate sodium (ALN) or with different doses of naringin markedly improved bone microarchitecture and increased bone mineral density (BMD). Trabecular morphology analysis showed that, relative to the sham group, the OVX group exhibited disordered trabecular arrangement, decreased trabecular thickness, and increased trabecular separation. Naringin treatment notably ameliorated these morphological abnormalities, with the high-dose naringin group showing the most pronounced improvement (Fig. 8A–F). Furthermore, serum levels of bone metabolism markers were measured. Compared with the sham group, the OVX model group displayed a significant increase in C-terminal telopeptide of type I collagen (CTX-1) and a decrease in N-terminal propeptide of type I procollagen (P1NP). Both ALN and naringin intervention significantly lowered serum CTX-1 levels and elevated P1NP levels, indicating that naringin can restore bone metabolic balance (Fig. 8G, H).

3.6. Naringin regulates autophagy, apoptosis, and the PI3K/AKT/mTOR pathway in bone tissue of ovariectomized mice

To assess the effects of naringin on autophagy and apoptosis in vivo, immunohistochemical analysis was performed on femoral tissues. Compared to the sham-operated group, the OVX group exhibited significantly reduced autophagy, as indicated by lower LC3 and higher P62 protein expression. Naringin treatment reversed these changes, enhancing LC3 and reducing P62 expression, which suggests that naringin activates autophagy in bone tissue (Fig. 9A–E). Concurrently, apoptosis levels were elevated in the OVX group, evidenced by increased expression of cleaved Caspase-3 and BAX. Naringin treatment effectively lowered the expression of these pro-apoptotic proteins (Fig. 9A–E).

We further examined whether naringin exerts these effects through the PI3K/AKT/mTOR pathway. Western blot analysis revealed that phosphorylation levels of PI3K, AKT, and mTOR were significantly higher in the OVX group than in the sham group. Naringin treatment markedly suppressed this OVX-induced hyperactivation of the pathway (Fig. 10A–D). Consistent with pathway inhibition, the OVX group showed suppressed autophagy (reduced LC3-II/LC3-I ratio and Beclin-1) and enhanced apoptosis (increased cleaved Caspase-3 and BAX, decreased Bcl-2). Naringin intervention significantly counteracted all these OVX-mediated alterations (Fig. 10E–J). In summary, these in vivo results demonstrate that naringin reactivates protective autophagy and inhibits excessive apoptosis in bone tissue, likely by suppressing the overactivated PI3K/AKT/mTOR signaling pathway.

Descargado para Lucia Angulo (lu.maru26@gmail.com) en National Library of Health and Social Security de ClinicalKey.es por Elsevier en octubre 15, 2026. Para uso personal exclusivamente. No se permiten otros usos sin autorización. Copyright ©2026. Elsevier Inc. Todos los derechos reservados.

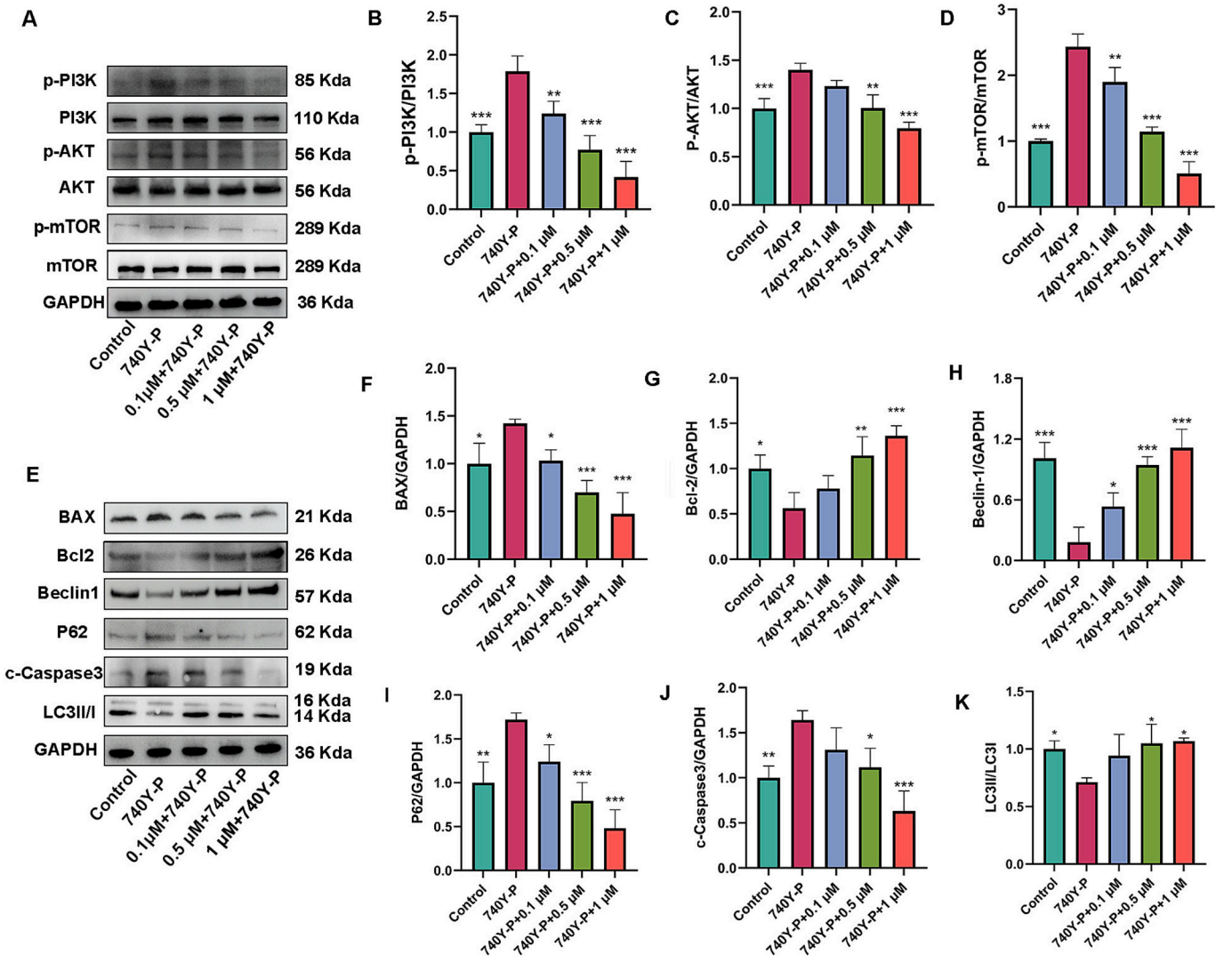


Fig. 6. Naringin regulates autophagy and apoptosis in MC3T3-E1 cells through the PI3K/AKT/mTOR pathway (n = 3). **A–D:** phosphorylation of PI3K/AKT/mTOR and total protein expression after treatment with naringin and 740Y-P; **E–K:** Expression of autophagy - and apoptosis-related proteins in MC3T3-E1 cells. * $P < 0.05$, ** $P < 0.01$, ***$P < 0.001$ compared with control.

4. Discussion

OP is a prevalent metabolic bone disease whose core mechanism lies in the imbalance between bone formation and resorption. The decline of osteoblast function, along with dysregulated apoptosis and autophagy, is closely associated with disease progression, posing a serious threat to bone health in the elderly, particularly postmenopausal women [24–26]. In recent years, natural flavonoids have garnered considerable attention for the prevention and treatment of OP due to their multi-target effects and favorable safety profiles [27,28]. Naringin, a dihydroflavonoid abundant in citrus plants and traditional herbs such as Drynaria fortunei, has demonstrated clear bone-protective activity. However, its mechanisms in regulating osteoblast autophagy and apoptosis remain to be fully elucidated [29–31]. Based on network pharmacology predictions and validation through in vitro and in vivo experiments, this study clarifies the core mechanism underlying the anti-osteoporotic effects of naringin, providing stronger theoretical support for its potential clinical translation.

In this study, multi-database integration identified 86 intersecting targets of naringin and OP. GO and KEGG enrichment analyses revealed that these targets were primarily enriched in biological processes such as intracellular receptor signaling and the regulation of inflammatory response, and were significantly associated with the PI3K/AKT/mTOR signaling pathway, as well as pathways related to apoptosis and autophagy. These predictions align with previous studies indicating that flavonoids can intervene in osteoporosis by modulating programmed cell death [3,32,33]. The PI3K/AKT/mTOR pathway serves as a central signaling axis regulating cell proliferation, differentiation, autophagy, and apoptosis, and its aberrant activation has been confirmed to lead to osteoblast dysfunction, thereby exacerbating OP progression [34]. The favorable binding affinity of naringin with AKT and PI3K, core components of this pathway, provides a biological basis for its direct targeting of this pathway.

The viability and function of osteoblasts are critical determinants of bone formation efficiency. As a cellular self-protection mechanism, autophagy enhances osteoblast adaptation to adverse microenvironments by clearing damaged organelles and maintaining metabolic homeostasis. Conversely, excessive apoptosis leads to osteoblast loss and exacerbates bone resorption [35,36]. Our in vitro experiments confirmed that naringin at concentrations of 0.1–1 μmol/L significantly promoted the proliferation and differentiation of MC3T3-E1 osteoblasts and upregulated the expression of osteogenic markers, including RUNX2, OPN, and OCN. These findings are consistent with previously reported bone-protective effects of naringin [12,37,38]. More

Descargado para Lucia Angulo (lu.maru26@gmail.com) en National Library of Health and Social Security de ClinicalKey.es por Elsevier en octubre 15, 2026. Para uso personal exclusivamente. No se permiten otros usos sin autorización. Copyright ©2026. Elsevier Inc. Todos los derechos reservados.

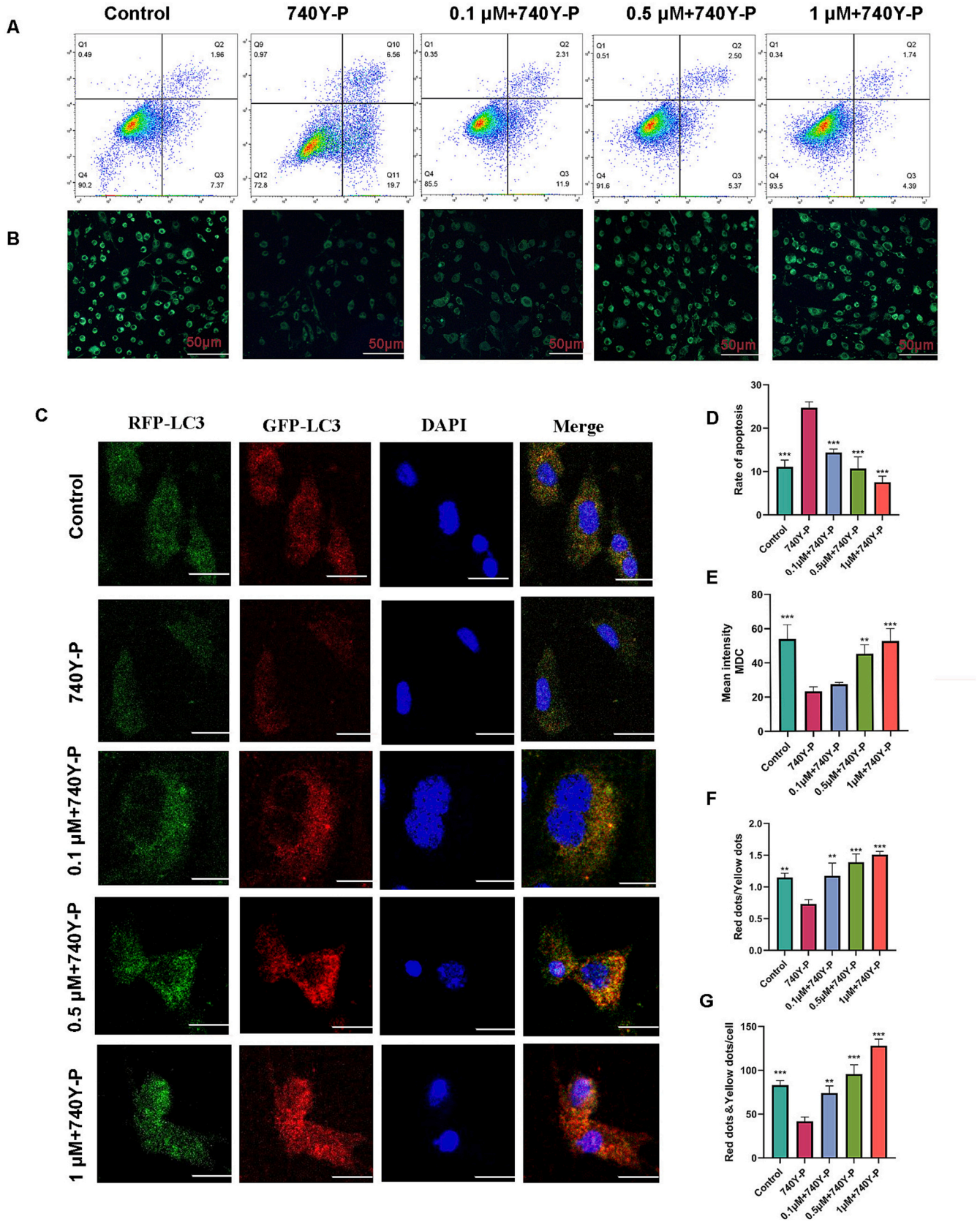


Fig. 7. Naringin regulates autophagy and apoptosis in MC3T3-E1 cells through the PI3K/AKT/mTOR pathway (n = 3). **A:** MDC staining was used to detect the level of autophagy. **B:** MC3T3-E1 cell apoptosis rate was detected by flow cytometry. **C:** mRFP-EGFP-LC3B was used to detect autophagic flux(Scale bar = 20 μm). **D** and **E** are the results of MDC and flow cytometry statistical analysis, respectively. **F** and **G** are quantitative analyses of mRFP-EGFP-LC3B. * $P < 0.05$, ** $P < 0.01$, ***$P < 0.001$ compared with control.

Descargado para Lucia Angulo (lu.maru26@gmail.com) en National Library of Health and Social Security de ClinicalKey.es por Elsevier en octubre 15, 2026. Para uso personal exclusivamente. No se permiten otros usos sin autorización. Copyright ©2026. Elsevier Inc. Todos los derechos reservados.

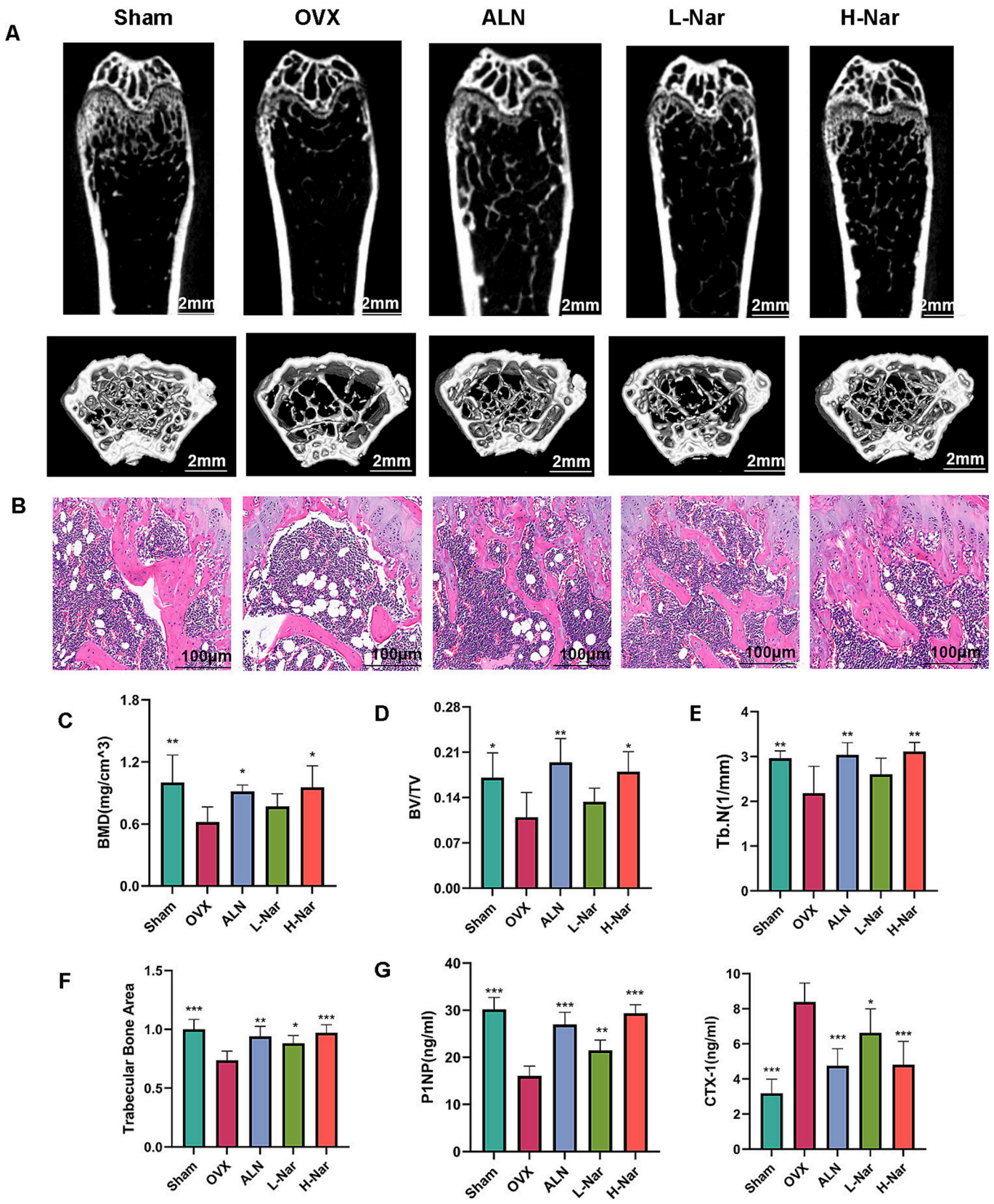


Fig. 8. Naringin increased bone mineral density and ameliorated osteoporosis in ovariectomized mice. **A:** Micro-CT of mouse distal femur tissue (n = 6); **B:** HE staining results of distal femur tissue of mice (n = 5); **C–E:** Bone mineral density and trabecular parameters of the distal femur tissue of mice; F: Statistical analysis results of HE staining; **G–H:** Expression levels of serum CTX-1、P1NP. * $P < 0.05$, ** $P < 0.01$, ***$P < 0.001$ compared with control.

Descargado para Lucia Angulo (lu.maru26@gmail.com) en National Library of Health and Social Security de ClinicalKey.es por Elsevier en octubre 15, 2026. Para uso personal exclusivamente. No se permiten otros usos sin autorización. Copyright ©2026. Elsevier Inc. Todos los derechos reservados.

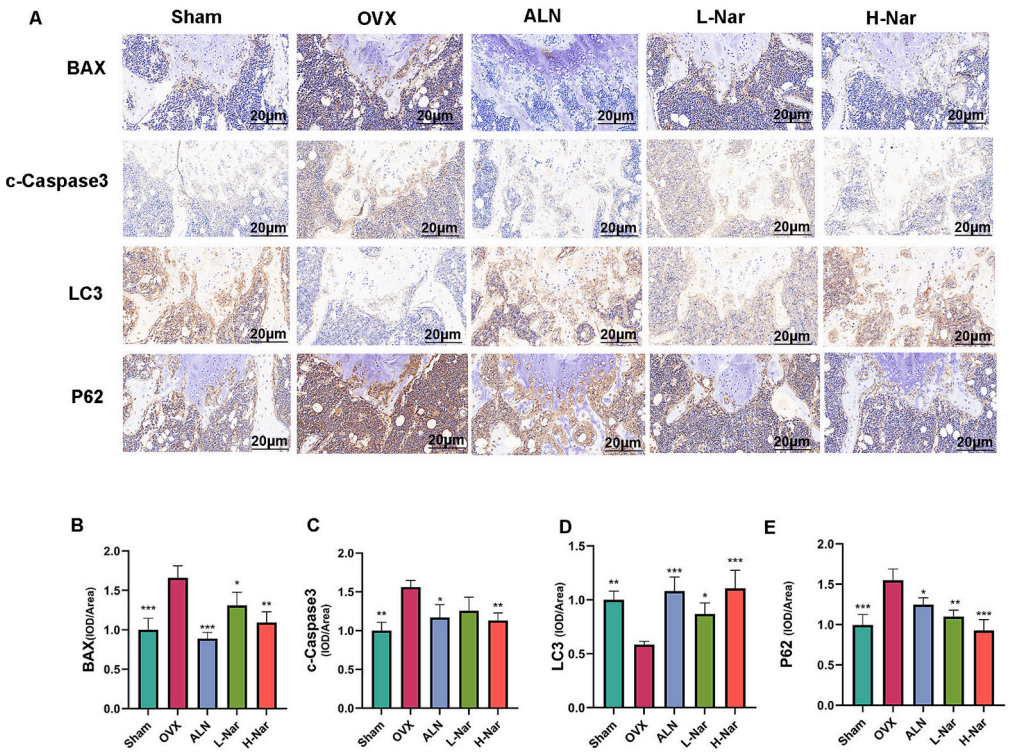


Fig. 9. Expression of autophagy and apoptosis-related proteins detected by immunohistochemical staining (n = 3). **A:** Immunohistochemical staining results; **B–E:** Results of immunohistochemical statistical analysis. * $P < 0.05$, ** $P < 0.01$, ***$P < 0.001$ compared with control.

importantly, naringin markedly increased the expression of autophagy-related proteins Beclin-1 and the LC3-II/LC3-I ratio, while reducing the accumulation of the autophagy substrate p62. Concurrently, it inhibited the expression of the pro-apoptotic proteins cleaved Caspase-3 and BAX and enhanced the expression of the anti-apoptotic protein Bcl-2.

To further verify the mediating role of autophagy activation in the anti-apoptotic effect of naringin, we employed the autophagy inhibitor 3-methyladenine (3-MA) [39]. The results demonstrated that 3-MA significantly reversed naringin-induced autophagy activation and its anti-apoptotic effect. This finding aligns with reports that moderate autophagy reduces osteoblast apoptosis and enhances their differentiation capacity [40,41], clearly indicating that naringin protects osteoblasts via autophagy activation.

This study further confirmed the central mediating role of the PI3K/AKT/mTOR pathway in naringin's regulation of osteoblast autophagy and apoptosis. Treatment with the PI3K activator 740Y-P significantly enhanced the phosphorylation of PI3K, AKT, and mTOR, which inhibited autophagy and promoted osteoblast apoptosis. Naringin dose-dependently reversed these effects, restoring autophagy and inhibiting apoptosis, thereby clarifying the specific involvement of this pathway. Consistent with our findings, numerous studies have shown that inhibition of the PI3K/Akt/mTOR pathway decreases mTOR activity, relieves autophagy suppression, and upregulates autophagy-related mRNA and protein expression, thereby enhancing autophagy in BMSCs and MC3T3-E1 cells [42–45]. The subsequent activation of autophagy-related genes promotes osteoblast differentiation and increases bone formation [46,47].

In vivo validation is essential for evaluating drug efficacy. The OVX mouse model is widely used for the in vivo assessment of anti-osteoporotic agents, as it closely mimics the pathological features of postmenopausal osteoporosis [48]. The present results demonstrated that naringin significantly improved bone microstructure, increased bone mineral density, downregulated the bone resorption marker CTX-1, and upregulated the bone formation marker P1NP in OVX mice, with a more pronounced effect at the higher dose. These findings confirm the potent anti-osteoporotic activity of naringin in vivo. Furthermore, immunohistochemical analysis revealed that naringin activated autophagy, suppressed apoptosis, and inhibited the overactivation of the PI3K/AKT/mTOR pathway in bone tissue, which closely aligned with the in vitro results. The consistency between in vivo and in vitro experiments strengthens the reliability of our conclusions.

Previous studies have indicated that naringin promotes osteogenic differentiation of bone marrow mesenchymal stem cells via the JAK2/STAT3 pathway, alleviates bone loss, and improves bone metabolism in osteoporotic rats [12]. Naringin has also been shown to upregulate Rspo1/Lgr4 expression, thereby enhancing bone formation through the Wnt/β-catenin signaling pathway and counteracting bone loss induced by mechanical unloading [49]. In contrast, the present study elucidates a novel mechanism by which naringin regulates osteoblast function through the PI3K/AKT/mTOR-autophagy-apoptosis axis. This suggests that naringin may exert its anti-osteoporotic effects via multiple pathways, providing a new perspective for comprehensively understanding the complexity of its bone-protective actions.

Although this study systematically elucidates the core mechanism by which naringin counteracts osteoporosis, certain limitations remain. The current investigation was limited to the OVX mouse model for efficacy validation; future studies should further examine its effects in other established models, such as aged or glucocorticoid-induced osteoporosis, to clarify its broader applicability. Additionally, the direct regulatory impact of naringin on osteoclast function was not examined and warrants targeted investigation in subsequent research.

5. Conclusions

In conclusion, through a combination of network pharmacology and in vitro and in vivo experiments, this study demonstrates for the first time that naringin improves osteoblast function and alleviates osteoporosis in ovariectomized mice by inhibiting the PI3K/AKT/mTOR pathway, thereby regulating autophagy and inhibiting osteoblast apoptosis. This work not only reveals a new molecular mechanism of

Descargado para Lucia Angulo (lu.maru26@gmail.com) en National Library of Health and Social Security de ClinicalKey.es por Elsevier en octubre 15, 2026. Para uso personal exclusivamente. No se permiten otros usos sin autorización. Copyright ©2026. Elsevier Inc. Todos los derechos reservados.

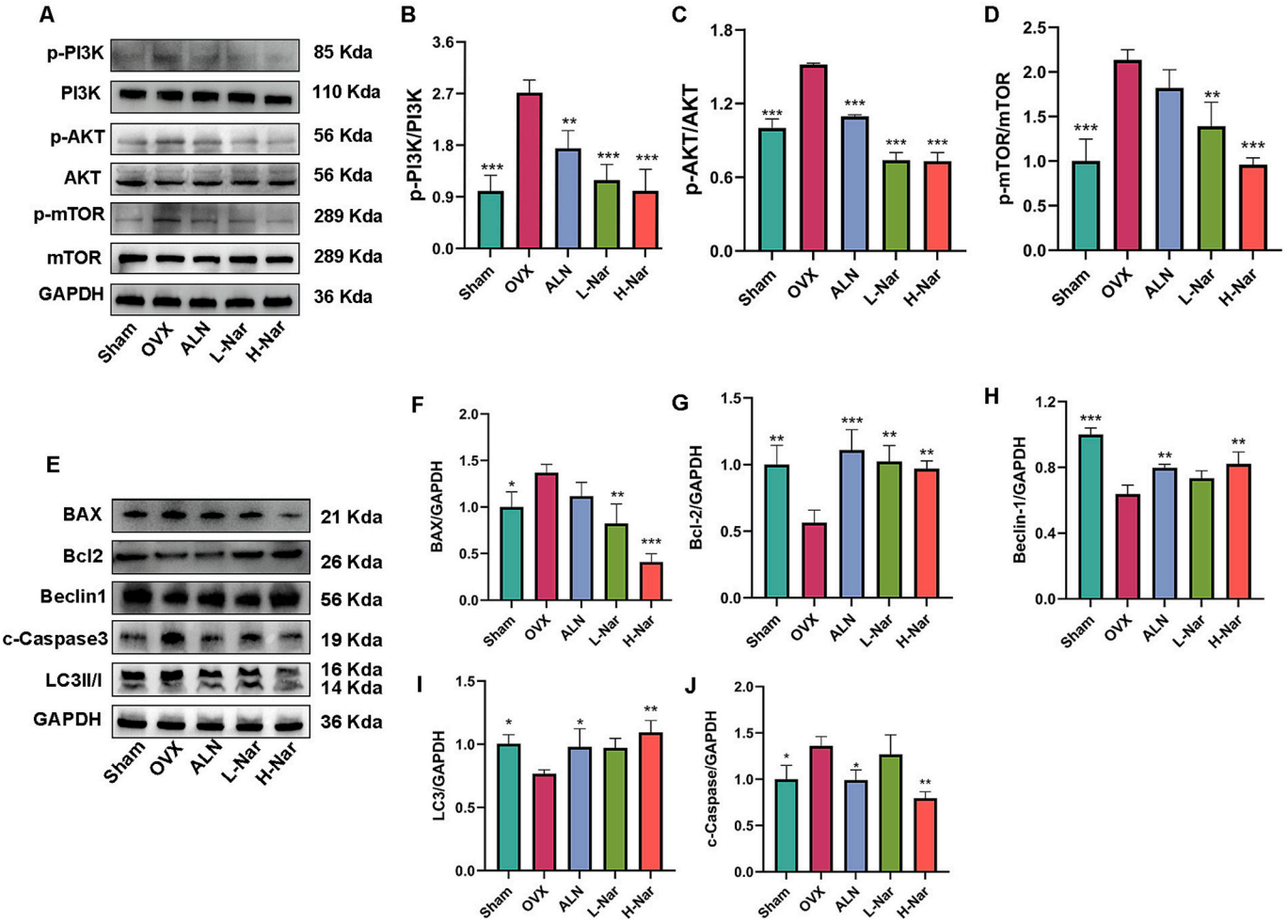


Fig. 10. Naringin regulates autophagy, apoptosis, and the PI3K/AKT/mTOR signaling pathway in vivo (n = 3). **A–D:** PI3K/AKT/mTOR phosphorylation and total protein expression; **E–K:** Expression of autophagy and apoptosis-related proteins. * $P < 0.05$, ** $P < 0.01$, ***$P < 0.001$ compared with control.

naringin against OP but also provides a rationale for the application of natural flavonoids in OP prevention and treatment. These findings position naringin as a potential candidate drug for clinical use, underscoring its theoretical significance and translational value.

CRediT authorship contribution statement

Yubo Cui: Writing – original draft, Visualization, Methodology, Investigation, Data curation. **Guisong Yu:** Writing – original draft, Visualization, Methodology, Investigation, Data curation. **Dian Li:** Visualization, Methodology, Investigation. **Xing Fu:** Visualization, Methodology, Investigation. **Zhijun Yang:** Methodology, Investigation. **Wenlong Yang:** Writing – review & editing, Investigation, Funding acquisition, Conceptualization. **Fengyun Yang:** Writing – review & editing, Investigation, Funding acquisition, Conceptualization.

Funding

This work was supported by the following grants:

- Natural Science Foundation of Jiangxi Province (20232BAB216116);
- Science and Technology Plan Project of Jiangxi Provincial Health Commission (Gan Cai She Zhi [2024] No. 8);
- Standardization Project of Jiangxi Provincial Traditional Chinese Medicine Standardization Committee (Gan TCM Biao Zi [2024] No. 1);
- Jiangxi Province Traditional Chinese Medicine Advantageous Disease (Knee Bi) Cultivation Project (Gan Cai She Zhi [2023] No. 70);
- Jiangxi Province College Students Innovation and Entrepreneurship Training Program (No. S202510412129/S202510412125);
- Graduate Student Innovation Program of Jiangxi Province (YC2024-B237/XJ-B202507).

Declaration of competing interest

The authors declare that they have no known competing financial interests or personal relationships that could have appeared to influence the work reported in this paper.

Descargado para Lucia Angulo (lu.maru26@gmail.com) en National Library of Health and Social Security de ClinicalKey.es por Elsevier en octubre 15, 2026. Para uso personal exclusivamente. No se permiten otros usos sin autorización. Copyright ©2026. Elsevier Inc. Todos los derechos reservados.

Data availability

Data will be made available on request.

References

[1] P. Subarajan, R.M. Arceo-Mendoza, P.M. Camacho, Postmenopausal osteoporosis: a review of latest guidelines, Endocrinol. Metab. Clin. N. Am. 53 (2024) 497–512, https://doi.org/10.1016/j.ecl.2024.08.008.

[2] F.F. Lyu, V. Ramoo, P.L. Chui, C.G. Ng, Y. Zhang, Prevalence rate of primary osteoporosis in China: a meta-analysis, BMC Public Health 24 (2024) 1518, https://doi.org/10.1186/s12889-024-18932-w.

[3] Z. An, B. Wu, W. Mao, L. Wu, Mechanisms and traditional Chinese medicine therapeutics for primary osteoporosis: an integrated perspective, Front. Endocrinol. (Lausanne) 16 (2025) 1638629, https://doi.org/10.3389/fendo.2025.1638629.

[4] T. Komori, Cell death in chondrocytes, osteoblasts, and osteocytes, Int. J. Mol. Sci. 17 (2016) 2045, https://doi.org/10.3390/ijms17122045.

[5] S. Nayak, S.L. Greenspan, A systematic review of combination treatment strategies for osteoporosis, JBMR Plus 9 (2025) ziaf165, https://doi.org/10.1093/jbmrpl/ziaf165.

[6] S. Davis, E. Simpson, J. Hamilton, M.M.-S. James, A. Rawdin, R. Wong, E. Goka, N. Gittoes, P. Selby, Denosumab, raloxifene, romosozumab and teriparatide to prevent osteoporotic fragility fractures: a systematic review and economic evaluation, Health Technol. Assess. 24 (2020) 1–314, https://doi.org/10.3310/hta24290.

[7] R.A. Adler, G. El-Hajj Fuleihan, D.C. Bauer, P.M. Camacho, B.L. Clarke, G.A. Clines, J.E. Compston, M.T. Drake, B.J. Edwards, M.J. Favus, S.L. Greenspan, R. McKinney, R.J. Pignolo, D.E. Sellmeyer, Managing osteoporosis in patients on long-term bisphosphonate treatment: report of a Task Force of the American Society for Bone and Mineral Research, J. Bone Miner. Res. 31 (2016) 16–35, https://doi.org/10.1002/jbmr.2708.

[8] T. Imatoh, K. Sai, M. Takeyama, K. Hori, M. Karayama, K. Furuhashi, K. Segawa, M. Kimura, J. Kawakami, Y. Saito, Identification of risk factors and development of detection algorithm for denosumab-induced hypocalcaemia, J. Clin. Pharm. Ther. 44 (2019) 62–68, https://doi.org/10.1111/jcpt.12753.

[9] P. Ramesh, R. Jagadeesan, S. Sekaran, A. Dhanasekaran, S. Vimalraj, Flavonoids: classification, function, and molecular mechanisms involved in bone remodelling, Front. Endocrinol. (Lausanne) 12 (2021) 779638, https://doi.org/10.3389/fendo.2021.779638.

[10] N. Benedetto, V. Carlucci, I. Faraone, L. Lela, M. Ponticelli, D. Russo, C. Mangieri, N.T. Tzvetkov, L. Milella, An insight into Citrus medica Linn.: a systematic review on phytochemical profile and biological activities, Plants (Basel) 12 (2023) 2267, https://doi.org/10.3390/plants12122267.

[11] Z. Zhu, W. Xie, Y. Li, Z. Zhu, W. Zhang, Effect of naringin treatment on postmenopausal osteoporosis in ovariectomized rats: a meta-analysis and systematic review, Evid. Based Complement. Alternat. Med. 2021 (2021) 6016874, https://doi.org/10.1155/2021/6016874.

[12] W. Wang, J. Mao, Y. Chen, J. Zuo, L. Chen, Y. Li, Y. Gao, Q. Lu, Naringin promotes osteogenesis and ameliorates osteoporosis development by targeting JAK2/STAT3 signalling, Clin. Exp. Pharmacol. Physiol. 49 (2022) 113–121, https://doi.org/10.1111/1440-1681.13591.

[13] S. Gera, S. Sampathi, S. Maddukuri, S. Dodoala, V. Junnuthula, S. Dyawanapelly, Therapeutic potential of naringenin nanosuspension: in vitro and in vivo anti-osteoporotic studies, Pharmaceutics 14 (2022) 1449, https://doi.org/10.3390/pharmaceutics14071449.

[14] D. Wang, W. Ma, F. Wang, J. Dong, D. Wang, B. Sun, B. Wang, Stimulation of Wnt/β-catenin signaling to improve bone development by naringin via interacting with AMPK and Akt, Cell. Physiol. Biochem. 36 (2015) 1563–1576, https://doi.org/10.1159/000430319.

[15] J.-B. Wu, Y.-C. Fong, H.-Y. Tsai, Y.-F. Chen, M. Tsuzuki, C.-H. Tang, Naringin-induced bone morphogenetic protein-2 expression via PI3K, Akt, c-Fos/c-Jun and AP-1 pathway in osteoblasts, Eur. J. Pharmacol. 588 (2008) 333–341, https://doi.org/10.1016/j.ejphar.2008.04.030.

[16] L. Yu, Y. Chen, S.A. Tooze, Autophagy pathway: cellular and molecular mechanisms, Autophagy 14 (2018) 207–215, https://doi.org/10.1080/15548627.2017.1378838.

[17] S. Nakamura, T. Yoshimori, New insights into autophagosome-lysosome fusion, J. Cell Sci. 130 (2017) 1209–1216, https://doi.org/10.1242/jcs.196352.

[18] S. Liu, S. Yao, H. Yang, S. Liu, Y. Wang, Autophagy: regulator of cell death, Cell Death Dis. 14 (2023) 648, https://doi.org/10.1038/s41419-023-06154-8.

[19] Y. Li, P. Yu, Y. Gao, Z. Ma, H. Wang, Y. Long, Z. Ma, R. Liu, Effects of the combination of Epimedii Folium and Ligustri Lucidi Fructus on apoptosis and autophagy in SOP rats and osteoblasts via PI3K/AKT/mTOR pathway, Biomed. Pharmacother. 173 (2024) 116346, https://doi.org/10.1016/j.biopha.2024.116346.

[20] Q. Zheng, Q.-C. Zhu, B.-K. Zhao, A.-L. Chen, Y. Tu, X.-J. Liu, From mechanisms to therapeutics: a narrative review on pyroptosis and autophagy in osteoporosis, Ann. Med. 57 (2025) 2599557, https://doi.org/10.1080/07853890.2025.2599557.

[21] D. Heras-Sandoval, J.M. Pérez-Rojas, J. Pedraza-Chaverri, Novel compounds for the modulation of mTOR and autophagy to treat neurodegenerative diseases, Cell. Signal. 65 (2020) 109442, https://doi.org/10.1016/j.cellsig.2019.109442.

[22] C. Jiang, Y. Wang, M. Zhang, J. Xu, Cholesterol inhibits autophagy in RANKL-induced osteoclast differentiation through activating the PI3K/AKT/mTOR signaling pathway, Mol. Biol. Rep. 49 (2022) 9217–9229, https://doi.org/10.1007/s11033-022-07747-w.

[23] J. Huang, Y. Ye, Y. Xiao, Q. Ren, Q. Zhou, M. Zhong, L. Jiao, L. Wu, Geniposide ameliorates glucocorticoid-induced osteoblast apoptosis by activating autophagy, Biomed. Pharmacother. 155 (2022) 113829, https://doi.org/10.1016/j.biopha.2022.113829.

[24] R. Chen, C. Yang, F. Yang, A. Yang, H. Xiao, B. Peng, C. Chen, B. Geng, Y. Xia, Targeting the mTOR-autophagy axis: unveiling therapeutic potentials in osteoporosis, Biomolecules 14 (2024) 1452, https://doi.org/10.3390/biom14111452.

[25] J.-M. Kim, C. Lin, Z. Stavre, M.B. Greenblatt, J.-H. Shim, Osteoblast-osteoclast communication and bone homeostasis, Cells 9 (2020) 2073, https://doi.org/10.3390/cells9092073.

[26] K.-Y. Chin, B.N. Ng, M.K.I. Rostam, N.F.D. Muhammad Fadzil, V. Raman, F. Mohamed Yunus, S.A. Syed Hashim, S.O. Ekeuku, A mini review on osteoporosis: from biology to pharmacological management of bone loss, J. Clin. Med. 11 (2022) 6434, https://doi.org/10.3390/jcm11216434.

[27] Y. Yang, N. Wang, X. Wang, J. Guo, B. Yang, X. Jia, L. Feng, Self-assembled nanomaterials from a holistic perspective of Chinese herbal medicine: accessibility and efficacy in anti-osteoporosis, Adv. Healthc. Mater. (2025) e04047, https://doi.org/10.1002/adhm.202504047.

[28] J. Li, X. Huang, Y. Yuan, H. Zhang, H. Zhou, W. Xiong, Y. Li, Z. Zhang, F. Qie, Y. Mao, B. Liang, X. Shi, K. Liu, Efficacy and safety of epimedium total flavonoids for primary osteoporosis: a systematic review and meta-analysis, Front. Pharmacol. 15 (2024) 1505926, https://doi.org/10.3389/fphar.2024.1505926.

[29] V.S. Shilpa, R. Shams, K.K. Dash, V.K. Pandey, A.H. Dar, S. Ayaz Mukarram, E. Harsányi, B. Kovács, Phytochemical properties, extraction, and pharmacological benefits of naringin: a review, Molecules 28 (2023) 5623, https://doi.org/10.3390/molecules28155623.

[30] M.A. Alam, N. Subhan, M.M. Rahman, S.J. Uddin, H.M. Reza, S.D. Sarker, Effect of citrus flavonoids, naringin and naringenin, on metabolic syndrome and their mechanisms of action, Adv. Nutr. 5 (2014) 404–417, https://doi.org/10.3945/an.113.005603.

[31] F. Li, X. Sun, J. Ma, X. Ma, B. Zhao, Y. Zhang, P. Tian, Y. Li, Z. Han, Naringin prevents ovariectomy-induced osteoporosis and promotes osteoclasts apoptosis through the mitochondria-mediated apoptosis pathway, Biochem. Biophys. Res. Commun. 452 (2014) 629–635, https://doi.org/10.1016/j.bbrc.2014.08.117.

[32] H. Hu, J. Zhang, X. Xin, Y. Jin, Y. Zhu, H. Zhang, R. Fan, Y. Ye, D. Li, Efficacy of natural products on premature ovarian failure: a systematic review and meta-analysis of preclinical studies, J. Ovarian Res. 17 (2024) 46, https://doi.org/10.1186/s13048-024-01369-5.

[33] P. Rao, F. Lou, D. Luo, C. Huang, K. Huang, Z. Yao, J. Xiao, Decreased autophagy impairs osteogenic differentiation of adipose-derived stem cells via Notch signaling in diabetic osteoporosis mice, Cell. Signal. 87 (2021) 110138, https://doi.org/10.1016/j.cellsig.2021.110138.

[34] F. Lou, T. Fu, Q. Li, P. Rao, S. Peng, S. Lu, T. Wu, Q. Li, J. Xiao, Activation of autophagy mediated by PI3K/Akt/mTOR signalling cascade alleviates impaired adipose-derived stem cell osteogenesis in a diabetic microenvironment, Br. J. Pharmacol. 182 (2025) 3522–3538, https://doi.org/10.1111/bph.70016.

[35] H. Cao, Q. Li, Y. Gao, J. Li, P. Yu, X. Lan, S. Peng, J. Xiao, Metformin promotes osteogenic differentiation of adipose-derived stem cells in diabetic osteoporosis by regulating autophagy, Cell Biol. Int. 49 (2025) 1354–1366, https://doi.org/10.1002/cbin.70061.

[36] S. Yang, Y. Lin, Y. Xie, T. Fu, T. Wu, X. Lan, F. Lou, J. Xiao, Empagliflozin ameliorates the impaired osteogenic differentiation ability of adipose-derived stem cells in diabetic osteoporosis by activating autophagy, Stem Cells 42 (2024) 623–635, https://doi.org/10.1093/stmcls/sxae019.

[37] H. Jiang, M. Zhang, X. Lin, X. Zheng, H. Qi, J. Chen, X. Zeng, W. Bai, G. Xiao, Biological activities and solubilization methodologies of naringin, Foods 12 (2023) 2327, https://doi.org/10.3390/foods12122327.

[38] G.-Y. Yu, G.-Z. Zheng, B. Chang, Q.-X. Hu, F.-X. Lin, D.-Z. Liu, C.-C. Wu, S.-X. Du, X.-D. Li, Naringin stimulates osteogenic differentiation of rat bone marrow stromal cells via activation of the notch signaling pathway, Stem Cells Int. 2016 (2016) 7130653, https://doi.org/10.1155/2016/7130653.

[39] T.-S. Xia, S.-Y. Xu, L.-Y. Lai, Y.-P. Jiang, N.-N. Wang, H.-L. Xin, Bitter acids from Humulus lupulus L. alleviate D-galactose induced osteoblastic senescence and bone loss via regulating AKT/mTOR-mediated autophagy, J. Food Drug Anal. 32 (2024) 506–519, https://doi.org/10.38212/2224-6614.3508.

[40] W. Liu, S. Xiang, Y. Wu, D. Zhang, C. Xie, H. Hu, Q. Liu, Icariin promotes bone marrow mesenchymal stem cells osteogenic differentiation via the mTOR/autophagy pathway to improve ketogenic diet-associated osteoporosis, J. Orthop. Surg. Res. 19 (2024) 127, https://doi.org/10.1186/s13018-024-04529-x.

[41] X. Zhang, J. Cui, L. Cheng, K. Lin, Enhancement of osteoporotic bone regeneration by strontium-substituted 45S5 bioglass via time-dependent modulation of autophagy and the Akt/mTOR signaling pathway, J. Mater. Chem. B 9 (2021) 3489–3501, https://doi.org/10.1039/d0tb02991b.

[42] B. Zhao, Q. Peng, E.H.L. Poon, F. Chen, R. Zhou, G. Shang, D. Wang, Y. Xu, R. Wang, S. Qi, Leonurine promotes the osteoblast differentiation of rat BMSCs by activation of autophagy via the PI3K/Akt/mTOR pathway, Front. Bioeng. Biotechnol. 9 (2021) 615191, https://doi.org/10.3389/fbioe.2021.615191.

[43] H.-X. Xiao, L. Yu, Y. Xia, K. Chen, W.-M. Li, G.-R. Ge, W. Zhang, Q. Zhang, H.-T. Zhang, D.-C. Geng, Sinomenine increases osteogenesis in mice with ovariectomy-induced bone loss by modulating autophagy, World J. Stem Cells 16 (2024) 486–498, https://doi.org/10.4252/wjsc.v16.i5.486.

[44] X. Li, Y. Zhu, X. Lin, C. Chen, H. Liu, Y. Shi, Beclin1- and Atg13-dependent autophagy activation and morroniside have synergistic effect on

Descargado para Lucia Angulo (lu.maru26@gmail.com) en National Library of Health and Social Security de ClinicalKey.es por Elsevier en octubre 15, 2026. Para uso personal exclusivamente. No se permiten otros usos sin autorización. Copyright ©2026. Elsevier Inc. Todos los derechos reservados.

osteoblastogenesis, Exp. Biol. Med. (Maywood) 247 (2022) 1764–1775, https://doi.org/10.1177/15353702221116879.
[45] L. C, Z. J, Y. Z, L. J, P. B, W. Z, Research on the role and mechanism of the PI3K/Akt/mTOR signalling pathway in osteoporosis, Front. Endocrinol. 16 (2025), https://doi.org/10.3389/fendo.2025.1541714.
[46] J. Wang, Y. Zhang, J. Cao, Y. Wang, N. Anwar, Z. Zhang, D. Zhang, Y. Ma, Y. Xiao, L. Xiao, X. Wang, The role of autophagy in bone metabolism and clinical significance, Autophagy 19 (2023) 2409–2427, https://doi.org/10.1080/15548627.2023.2186112.
[47] S. Wang, Z. Deng, Y. Ma, J. Jin, F. Qi, S. Li, C. Liu, F.-J. Lyu, Q. Zheng, The role of autophagy and mitophagy in bone metabolic disorders, Int. J. Biol. Sci. 16 (2020) 2675–2691, https://doi.org/10.7150/ijbs.46627.
[48] J. Plank, A. Damerau, M.S. Chacon, P. Hoff, F. Buttgereit, M. Pfeiffenberger, Modelling osteoporosis in pre-clinical research-challenges, trends and new approaches, Cells 14 (2025) 1649, https://doi.org/10.3390/cells14211649.
[49] G.-X. Shi, W.-D. Sun, Z.-H. Chen, C.-J. Yang, W.-L. Luo, D.-F. Wang, Z.-Z. Zhou, Drynaria Naringin alleviated mechanical stress deficiency-caused bone loss deterioration via Rspo1/Lgr4-mediated Wnt/β-catenin signalling pathway, In Vitro Cell. Dev. Biol. Anim. 59 (2023) 706–716, https://doi.org/10.1007/s11626-023-00815-w.

Descargado para Lucia Angulo (lu.maru26@gmail.com) en National Library of Health and Social Security de ClinicalKey.es por Elsevier en octubre 15, 2026. Para uso personal exclusivamente. No se permiten otros usos sin autorización. Copyright ©2026. Elsevier Inc. Todos los derechos reservados.